buildings

MDPI

Article

Induced Partial Saturation Using *Pseudomonas stutzeri* Biogas for Mitigate Structure Settlement

Meitong Lv [1,2], Dingwen Zhang [1,*], Erxing Peng [3] and Yinhe Guo [1]

[1] Institute of Geotechnical Engineering, Southeast University, Nanjing 210096, China; 230189833@seu.edu.cn (M.L.)
[2] Institute of Civil Engineering, Anhui Polytechnic University, Wuhu 241000, China
[3] Northwest Institute of Eco-Environment and Resources, Chinese Academy of Sciences, Lanzhou 730000, China
* Correspondence: zhang@seu.edu.cn

Abstract: Induced partial saturation (IPS) is a new foundation treatment method for mitigating soil liquefaction using biogas. A series of laboratory tests were performed to demonstrate the influencing factors of IPS using *Pseudomonas stutzeri* biogas. On the basis of the optimal biogas production conditions, the intervention effect of *Pseudomonas stutzeri* biogas on the foundation deformation under buildings was investigated based on shaking table tests. The test results showed that the best carbon source in the denitrification process of *Pseudomonas stutzeri* biogas is sodium citrate. The most effective initial value of optical density-based concentration was 0.1. The carbon–nitrogen ratio (C/N) of the bacterium suspension was used as the index to control the saturation. The degree of saturation reduction showed a good linear correlation with the C/N. The optimum temperature of this method was between 20 °C and 30 °C. The most suitable pH value was between 7 and 9. The environmental factors had minimal influence on the degree of saturation reduction but had a significant effect on the average rate of gas generation and the period of initial stagnation. After *Pseudomonas stutzeri* biogas desaturation, the settlement of the building was greatly reduced. The settlement of saturation of 92.5% sand foundation reached 17.1 mm, and the 85% saturation was only 10.6 mm. These results provide a good foundation for the feasibility of utilizing *Pseudomonas stutzeri* biogas mitigation of the liquefaction hazard of sand.

Keywords: desaturation; *Pseudomonas stutzeri*; biogas; environmental factors; settlement

Citation: Lv, M.; Zhang, D.; Peng, E.; Guo, Y. Induced Partial Saturation Using *Pseudomonas stutzeri* Biogas for Mitigate Structure Settlement. *Buildings* **2024**, *14*, 484. https://doi.org/10.3390/buildings14020484

Academic Editor: Eugeniusz Koda

Received: 28 December 2023
Revised: 7 February 2024
Accepted: 7 February 2024
Published: 8 February 2024

1. Introduction

Liquefaction refers to the loss of shear strength in fully saturated sand owing to an excess build-up of pore pressure during dynamic excitation, such as an earthquake [1–3]. Liquefaction-induced damages have been observed globally in the aftermath of moderate to large earthquakes. Damaging earthquakes occurred in 1992 in Landers, in 2011 in Tohoku-Oki, and in 2018 in Indonesia [4–8]. Therefore, studies related to liquefaction have become important in the field of geotechnical engineering [9,10]. Evaluating liquefaction hazards can reduce casualties caused by earthquakes [11,12]. Traditional liquefiable foundation treatment methods include sand compaction piles, gravel piles, cement–soil deep mixing columns, and others [13–15]. However, the existing treatment methods are only used for newly built foundations. Figure 1 shows pictures of buildings collapsing due to seismic liquefaction. Although the buildings have maintained their integrity, the buildings as a whole have tilted, settled, or rotated. As a result, the buildings could no longer be used and had to be demolished. This is a great waste of resources and great damage to the environment. Therefore, it effectively deals with liquefiable foundations under buildings, which becomes one of the key technical challenges.

(**a**) (**b**)

Figure 1. Building collapses due to earthquake liquefaction. (**a**) Niigata earthquake in Japan in 1964, (**b**) Taiwan earthquake in 1999.

Yoshimi et al. [16] put forward that the liquefaction resistance significantly increases with the decrease in saturation. With a desaturation of 70%, the liquefaction resistance of the sand was three times that of fully saturated sands. Okamura and Teraoka [17] conducted shaking table tests to study the gas desaturation to mitigate liquefaction. The test showed that the settlement of the model structure decreases from 48 mm to 8 mm, and the excess pore pressure decreases by nearly half from 100 kpa to 50 kpa when the sand saturation decreases to 98% [18]. Based on these findings, researchers have proposed the induced partial saturation (IPS) technology [19–22], hereinafter referred to as IPS technology. This new technology introduces the idea that by injecting a small number of bubbles into a liquefiable sand layer, the saturation of soil will decrease. During experimental testing, when liquefiable sand layers are subjected to seismic loads, bubbles can effectively reduce the increase in excess pore pressure. This technology can be used not only in new projects but also for upgrading existing buildings or structures. Okamura et al. [17] executed an air-injection technique in situ. The situ soil samples were collected, and the saturation ranged between 65% and 88% using field monitoring. Meanwhile, the long-term durability of introduced bubbles has been confirmed [23–25]. In accordance with the gas injection method, the existing IPS technology can be divided into air injection, water electrolysis, drainage recharge, and biogas [26,27]. Among these injection types, the biogas method mainly refers to the formation of bubbles using bacterial denitrification. The final product of denitrification is nitrogen, which is a non-toxic and safe inert gas. He et al. [28] purified mixed bacteria dominated by *Pseudomonas denitrificans* from activated sludge and studied the denitrification abilities and biogas generation efficiency of this bacterium. Then, He et al. [27] confirmed that nitrogen bubbles that were produced by bacteria can effectively reduce the saturation and improve the liquefaction resistance of soil through triaxial testing. Larger scale experiments, including field trials on microbial-induced desaturation, have been performed [29,30]. Li [31] pointed out that nitrogen bubbles lacked stability under the conditions of groundwater seepage and, therefore, proposed a new method to deal with the liquefaction resistance of liquefiable soil. This new method was based on a combination of biological gas and plugging.

Pseudomonas denitrificans was the major bacterium used in a previous biogas method. According to the research results, ethanol and sodium acetate are more suitable than methanol as the carbon source of bacteria. However, ethanol is flammable, volatile, and difficult to use in practical engineering [26,31]. *Pseudomonas stutzeri* is a Gram-negative, rod-shaped, motile, and non-fluorescent denitrifying bacterium, and it is commonly used

in aquaculture and sewage treatments [32]. *Pseudomonas stutzeri* has a strong denitrification capacity, and its optimal carbon source is sodium citrate, which is soluble in water and is non-volatile. *Pseudomonas stutzeri* can be used in IPS for mitigation liquefaction [33–36]. Peng et al. [33] induced partially saturated sand by the microbial denitrification process of *Pseudomonas stutzeri*. According to previous related studies, no research reported the use of *Pseudomonas stutzeri* to explore the impact of environmental factors on saturation reduction. To prove the feasibility of *Pseudomonas stutzeri*, control parameters of desaturation were analyzed, including temperature, pH, and type of soil. Finally, application conditions for the use of *Pseudomonas stutzeri* biogas were identified. On the basis of the optimal biogas production conditions, the intervention effect of *Pseudomonas stutzeri* biogas on the foundation deformation under the buildings was investigated based on shaking table tests. The conclusions can potentially provide a theoretical basis for the feasibility of utilizing *Pseudomonas stutzeri* biogas mitigation in the liquefaction of saturated sand.

2. Materials and Methods

2.1. Materials

2.1.1. Test Sand

The sand used was from a site in Jiangsu Province. The silt came from a site in Shandong Province. Table 1 summarizes the gradation parameters of sand. The maximum and minimum void ratios of sand are 0.946 and 0.428, respectively. The plastic and liquid limits of silt are 23.4% and 30.8%, respectively, and the plasticity index is 7.4. The soil was classified as poorly graded sand in accordance with the USCS (ASTM D2487). The silt was named low-liquid-limit silt in accordance with GB/T 50145-2007.

Table 1. Typical engineering properties of sand and silt.

Types of Soil	Specific Gravity G_s	Effective Grain Size D_{10}/mm	Median Particle Size D_{30}/mm	Mean Particle Size D_{50}/mm	Limiting Particle Size D_{60}/mm	C_u	C_c
Sand	2.68	0.27	0.33	0.42	0.46	1.71	0.88
Silt	2.79	-	0.0064	0.013	0.017	-	-

2.1.2. Bacterial Culture

Pseudomonas stutzeri denitrifying bacterium was used in this experiment, and it was purchased from a German microbial collection (DSMZ, 5190). Details of bacterial culture can be found in the work of Peng et al. [33]. The apparatus for bacterial culture is shown in Figure 2. *Pseudomonas stutzeri* was isolated and purified using plate streaking. The morphology of a single colony formed on the plate medium is shown in Figure 3. A single colony was then propagated and cultivated in an LB medium to obtain a pure strain of *Pseudomonas stutzeri*. The composition of denitrifying cultivation of the bacterium is as follows: magnesium sulfate heptahydrate ($MgSO_4 \cdot 7H_2O$) (0.2 g/L), potassium nitrate (KNO_3) (2 g/L), potassium hydrogen phosphate (K_2HPO_4) (1 g/L), and sodium citrate dihydrate ($Na_3C_6H_5O_7 \cdot 2H_2O$) (5 g/L). The electron donor in denitrification was sodium citrate, and potassium nitrate was the electron acceptor. The carbon–nitrogen ratio (C/N) was varied to obtain the target degree of saturation. Based on the principle of control variables, the concentration of KNO_3 in the denitrification medium was adjusted in each test. The concentrations of other tiny amounts of nutrients were unchanged. Nitrogen is a chemically inactive gas, and it has a very low solubility in water. The bubbles from direct injection are unstable, and they form the soil with a saturation gradient. Compared with hydrogen from the electrolysis method, nitrogen is not easy to burn and is safer to use.

(**a**) (**b**)

Figure 2. Bacterial culture instrument. (**a**) Sterilization pot, (**b**) aseptic operation table.

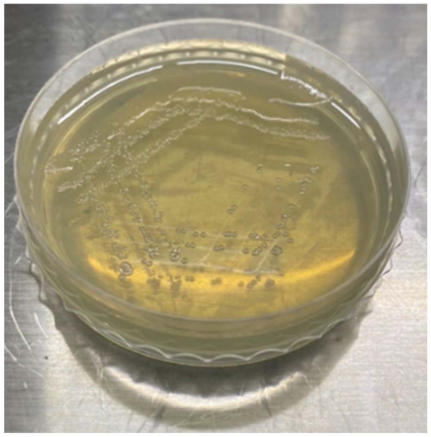

Figure 3. Colony morphology.

2.2. Methods

2.2.1. Denitrification Performance Verification

The concentration of potassium nitrate was varied to obtain the target saturation, and the denitrification ability of the bacterium was confirmed through the content changes of nitrate and nitrite. Optical density value (OD_{600}) was measured with a spectrophotometer whose type is HALO NDA master. The concentrations of nitrate and nitrite were detected using a Dionex ICS-1500 ion chromatography system. The instruments used are shown in Figure 4. The details of the verification procedures are as follows:

1. Luria–Bertani culture medium was used for bacterial growth. When the bacteria were in the logarithmic phase, they were centrifuged at 4000 r/min, and the supernatant was removed. Denitrification media was added to form a treatment solution with an OD_{600} equal to 0.1.
2. Then, 1 mL treatment liquid was added to 2 mL centrifuge tubes. According to the website DSMZ, static culture was performed at an optimal temperature of 30 °C.
3. Samples were obtained at 3 h intervals, and the concentrations of nitrate and nitrite were detected.

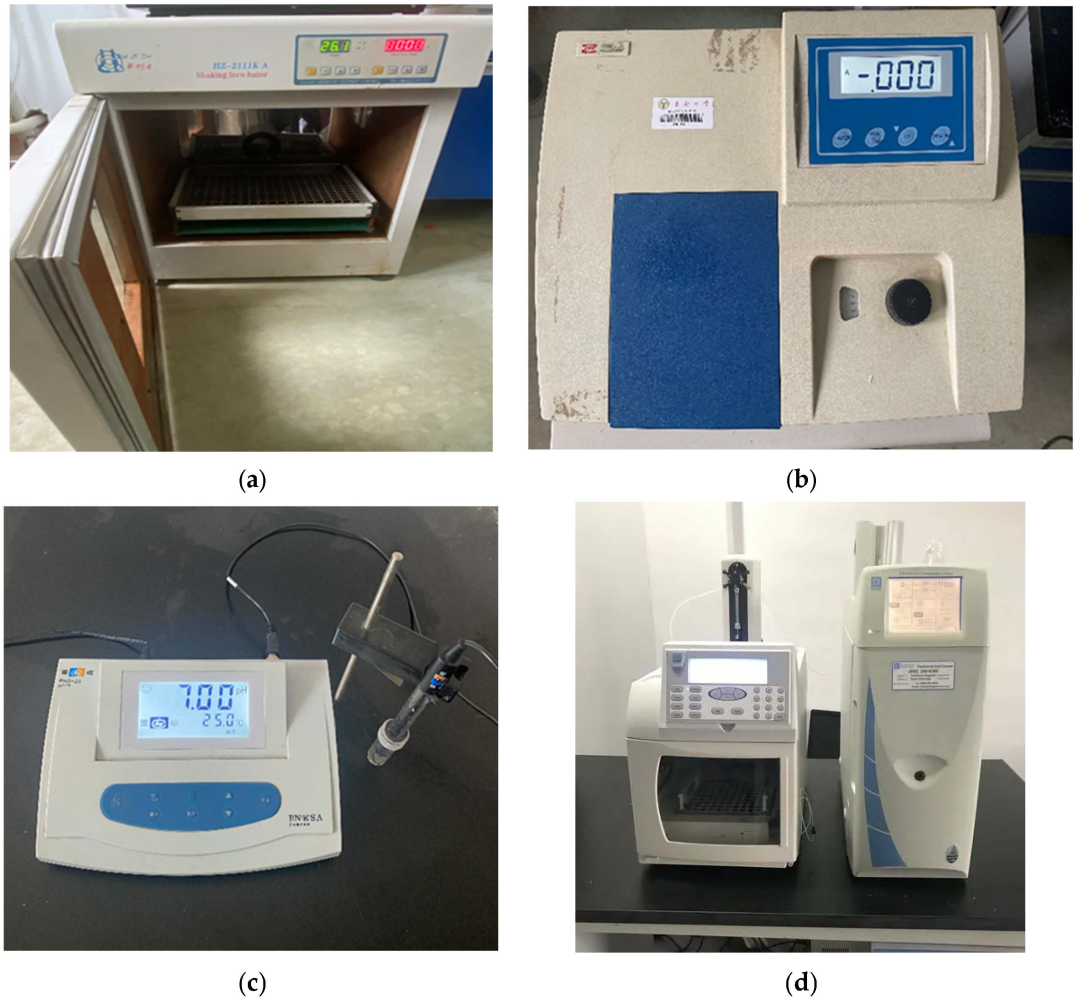

Figure 4. Test instruments. (**a**) Thermostatic incubator, (**b**) spectrophotometer, (**c**) pH meter, (**d**) Dionex ICS-1500 ion chromatography system.

2.2.2. Gas Generation Test

The gas-measuring device included the following: a 20 Ml syringe, 4 mm × 6 mm (inner diameter × outside diameter) PVC hoses, a 2 Ml glass pipette, and filter papers. The cylinder and handspike rod of the syringe required glue to achieve a tight bond. The schematic diagram of the measuring device is shown in Figure 5.

The preparation of sand samples was performed as follows: The treatment liquid was prepared with an OD_{600} of 0.1, as described in Section 2.2.1. The dry sand weight was calculated based on the specific gravity, sample volume, and dry density of soil particles. A certain amount of denitrification medium was added to the dry sand, and the resulting mixture was boiled to exhaust the air and then cooled in a beaker. The exhausted sand was mixed with a bacterial suspension of pure culture to form the treatment liquid with an OD_{600} of 0.1. For sand samples, the treatment liquid was first poured into the syringe, and sand was slowly deposited into the liquid. A saturated sample was prepared in the syringe.

The target volume and pore ratio of the samples were 10 cm^3 and 0.5, respectively. During the reaction, the generated gas shifted the level of liquid in the burette, which was measured at intervals of 6 h on the first day and at intervals of 12 h afterward. The concentration of total inorganic nitrogen (TIN) and ammonium in the pore water was tested after the bacteria had produced gas.

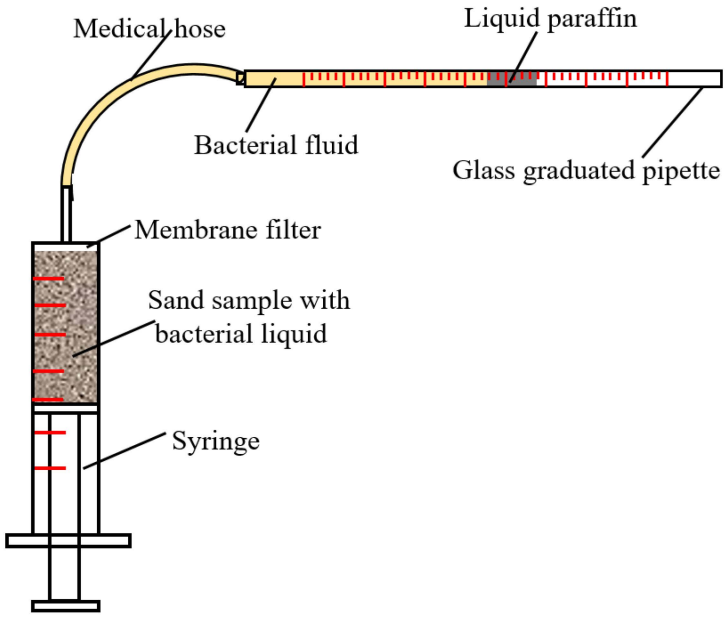

Figure 5. Schematic of gas measurement device.

2.2.3. Shaker Table Tests

The model foundation is a horizontal layer with dry sand on the top layer and a saturated sand layer at the bottom, as shown in Figure 6. The tests were prepared using the water-sinking method, ensuring that the sand samples were kept below the water surface at all times. The density of the foundation was controlled to be 40%. The building is made of Plexiglas panels and is based on a prototype three-story concrete frame structure with a similar ratio of 1:40. The vertical deformation of the building was monitored using a laser displacement meter fixed to a rigid support on the shaker table.

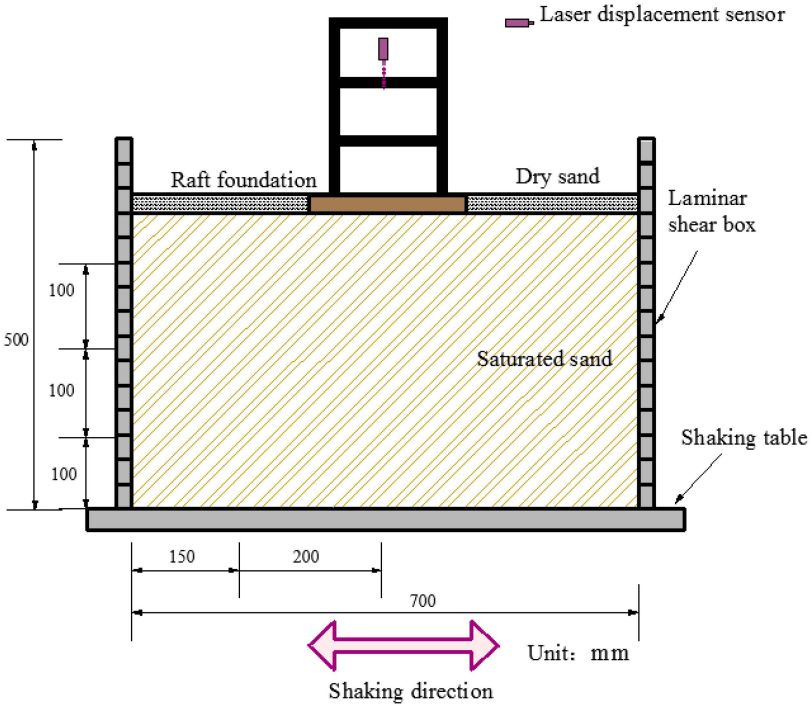

Figure 6. Section diagram of shaker table test.

2.3. Experimental Scheme of Gas Generation Test

Table 2 shows the details of the parameters related to the gas generation test. Each experiment was repeated in three groups, and the same bacterial suspension was used. Except for Study #3, the test temperature was room temperature. The temperatures were maintained between 25 °C and 30 °C.

Table 2. Summary scheme of gas generation test.

No.	Soil	Carbon Source	Bacterial Concentrations (OD_{600})	Nitrate Concentrations (mmol/L)	Temperature/°C	pH
1	100% Sand	Sodium citrate, Sodium acetate, Glucose	0.1	19.80	Room temperature	7
2	100% Sand	Sodium citrate	0.01, 0.05, 0.1, 0.15, 0.2	19.80	Room temperature	7
3	100% Sand	Sodium citrate	0.1	9.90, 14.85, 19.80, 29.70 and 39.60	Room temperature	7
4	100% Sand	Sodium citrate	0.1	19.80	4, 15, 20, and 30	7
5	100% Sand	Sodium citrate	0.1	19.80	Room temperature	5, 6, 7, 8, and 9
6	100% Sand, 99% Sand + 1% Silt 95% Sand + 5% Silt, 90% Sand + 10% Silt 75% Sand + 25% Silt	Sodium citrate	0.1	9.80	Room temperature	7

Studies #1, #2, and #3: Desaturation control. In Study #1, sodium citrate, sodium acetate, and glucose were used as carbon sources to prepare denitrification medium. The optimum carbon source for the test was determined from the nitrate and nitrite concentrations and the growth curve of the bacteria during the test. In Study #2, the microbial suspension was transferred to different initial bacterial concentrations to prepare the saturated sample. The effects of the initial concentration on the reduction in saturation were investigated. In addition, the optimal concentration of bacteria was confirmed. In Study #3, the optimal concentration of bacteria, which was determined in Study #2, was selected as the initial concentration of bacterial suspension. Different concentrations of nitrate were selected for microbial suspension. The effects of nitrate concentrations on desaturation were analyzed. Then, the relationship between the control parameters and the degree of saturation was proposed.

Studies #4, #5, and #6: Influencing factors. In accordance with the test results of Studies #2 and #3, the bacterial suspension was prepared with OD_{600} and nitrate concentrations of microbial suspension of 0.1 and 19.80 mmol/L, respectively. The desaturation of soil was determined under different conditions. In Study #5, 100% sand was replaced with a mixture of sand and silt, and the test steps were consistent with those of others.

The effects of various factors on the gas generation tests were analyzed in accordance with an assessment index composed of the degree of saturation reduction, the average rate of gas generation, and the initial stagnation of gas generation.

The average gas generation rate was calculated as follows:

$$\overline{v} = \frac{Q}{t_f - t_0} \quad (1)$$

where Q is the total amount of gas generation, t_0 is the initial time of gas generation, and t_f is the final time of gas generation.

When the microbial reaction process was completed, the saturation was calculated using the following formula:

$$S_r = \frac{V_v - V_a - V_{a0}}{V_v} = 1 - \frac{V_a}{V_v} - (1 - S_{r0}) = S_{r0} - \frac{V_a}{V_v} = S_{r0} - \frac{V_a}{V\frac{e}{1+e}} \quad (2)$$

where S_r is the sample saturation, V_v is the pore volume, V_a is the bacterial gas production, V_{a0} is the initial gas content, S_{r0} is the initial saturation, V is the sample volume, and e is the void ratio.

On the basis of the optimal biogas production conditions, shaker tests were carried out, and the test program is shown in Table 3. The sinusoidal waveform is the chosen load which has a frequency of 2 Hz and a peak acceleration of 0.2 g over a period of 20 s.

Table 3. Summary scheme of shaker table tests.

No.	Soil	Desaturation/%	Relative Density/%	Carbon Source	Temperature/°C	pH
1	100% Sand	100	40	Sodium citrate	25	7
2	100% Sand	92.5	40	Sodium citrate	25	7
3	100% Sand	85	40	Sodium citrate	25	7

3. Results and Discussion

3.1. Standard Curve of the Nitrates and Nitrites

The relationship between nitrate concentration and peak area can be obtained by fitting as follows: y = 1.7411x − 0.1684. Nitrite satisfies the relationship as follows: y = 2.2505x + 0.0311. The correlation coefficients of the fitted curves all reached 0.999. Trend analysis of nitrate and nitrites during the test by fitting the standard curve of nitrate and nitrites.

3.2. Control Method of Desaturation

3.2.1. Carbon Source Optimization

The concentration of nitrate and nitrites during the test was analyzed by fitting the standard curve of nitrate and nitrites. At the same time, the growth curve of bacteria during the test was recorded. Figure 7 shows the variation in the concentration of nitrate and nitrites and the growth curve of bacteria when IPS technology is performed using different carbon sources.

When potassium nitrate was used as the electron acceptor, and sodium citrate, sodium acetate, and glucose were used as the electron donor, the theoretical equations for the reaction of denitrification were as follows:

$$5C_5H_5O_5COO^{3-} + 18NO^{3-} \rightarrow 30CO_2\uparrow + 9N_2\uparrow + 6H_2O + 23OH^- \quad (3)$$

$$5CH_3COO^- + 8NO^{3-} \rightarrow 10CO_2\uparrow + 4N_2\uparrow + H_2O + 13OH^- \quad (4)$$

$$5C_6H_{12}O_6 + 24NO^{3-} \rightarrow 18CO_2\uparrow + 12N_2\uparrow + 30H_2O + 12CO_2{}^{2-} \quad (5)$$

It is observed from Figure 7a that following a culturing period of 21 h, the removal rate of nitrate reached 100% when sodium citrate was used as a carbon source. When the other two were used as carbon sources, they could not reach 100% within 34 h. When sodium acetate is used as the carbon source, the nitrate concentration is reduced to 40.3% at 34 h. In contrast, the reduction rate was only 11.12% at 34 h when glucose was used. Moreover, as indicated in Figure 7b, during the reduction process, accompanied by the accumulation of nitrite, the nitrite concentration reached its peak of 5.74 mmol/L at 18 h when sodium citrate was used as a carbon source. However, nitrite concentration reduced sharply to 0.74 mmol/L when the culturing period reached 21 h and was maintained near that value afterward. When sodium acetate was used as the carbon source, nitrite continued to accumulate up to a concentration of 8.41 mmol/L at 34 h. Acetate inhibited the activity

of nitrite reductase. Figure 7c shows that the bacteria proliferate quickly under a culture temperature of 30 °C (official optimum temperature), and they have a strong denitrification effect when sodium citrate is used as a carbon source. The effect of glucose on the reaction of nitrite reductase and nitrous oxide reductase was weaker than that of sodium citrate and sodium acetate, and it coincided well with Henderson et al. [37]. In conclusion, the best carbon source in the denitrification process of *Pseudomonas stutzeri* is sodium citrate.

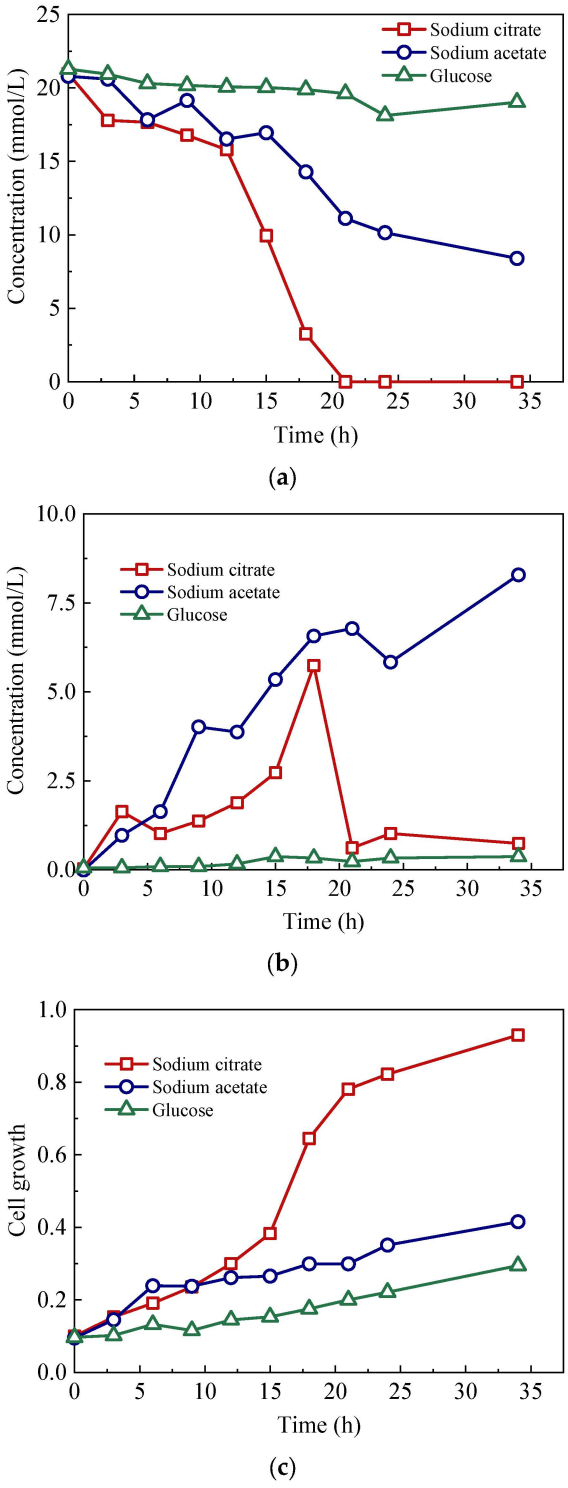

Figure 7. Denitrification conditions and growth curve of bacteria, (**a**) nitrate concentration, (**b**) nitrite concentration, (**c**) cell growth.

3.2.2. Bacterial Concentrations

Figure 8 shows the desaturation curves of the samples with different initial bacterial concentrations. The reduction extent of the degree of saturation first increased and then decreased when the initial OD_{600} increased from 0.01 to 0.2. When the OD_{600} was 0.1, the reduction extent of the saturation reached its highest, and the gas generation rate was the fastest. Furthermore, the initial stagnation was the shortest due to the direct effect of the amount of microbial inoculation on bacterial survival. Within a certain range, the greater the amount of inoculation, the higher the microbial activity and the faster the metabolic rate. However, the constant increase in the amount of inoculation led to a relative lack of nutrients, which resulted in mutual competition among bacteria. This result reduced the biological activities and decelerated metabolism [38]. Therefore, the optimal OD_{600} of the bacterial suspension was 0.1.

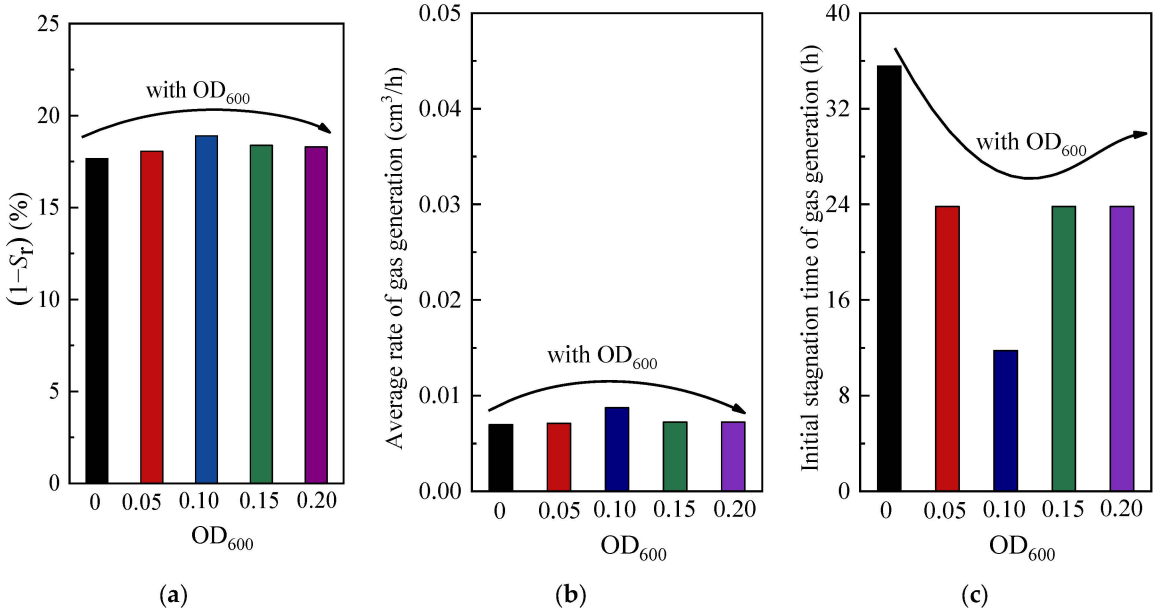

Figure 8. Desaturation curves with different bacterial concentrations. (**a**) $(1 - S_r)$, (**b**) average rate of gas generation, (**c**) initial stagnation of gas generation.

3.2.3. Nitrate Concentrations

Figure 9 shows the desaturation curves with different initial nitrate concentrations. It shows that when the concentration of nitrate increased from 9.9 mmol/L to 39.6 mmol/L, the reduction in saturation showed an increase.

Figure 10 shows the theoretical and test values of desaturation with different nitrate concentrations. The theoretical value was calculated under the condition that the total nitrate was completely translated into nitrogen. The figure shows that the test relationship curve did not constitute a linear relationship. By considering 14.85 mmol/L as the demarcation point of nitrate concentration, the relationship curve can then be divided into two parts, namely, an electron donor-deficient area and an electron donor-insufficient area. Then, in comparison with the 14.85 mmol/L concentration, the difference between the relationship curve and theoretical line in the two areas was larger. In the electron donor-deficient area, this result may have been due to the effect of C/N on nitrate removal by denitrification and ammonification of bacteria. When nitrate is treated as a substrate for denitrification, two forms of nitrate reduction occur, according to the research [39]. The first is the reduction in nitrate in the environment through the direct path of ammonification, whose product is ammonia. The second form is the indirect path of respiratory denitrification, in which case the products may be nitric oxide, nitrous oxide, and nitrogen gas. The relative contribution of ammonification and denitrification is a function of the C/N. Denitrification dominates environments that are rich in nitrates but are relatively deficient in electron

donors. Ammonification is largely favorable in electron-rich environments where only low concentrations of nitrates are available [40]. Therefore, the sample was dominated by ammonification reactions in this area. In the electron donor insufficient area, denitrification dominated the environment. However, the C/N was extremely low. The lack of an electron donor led to a low conversion rate of the TIN, which resulted in a decreased efficiency of gas generation.

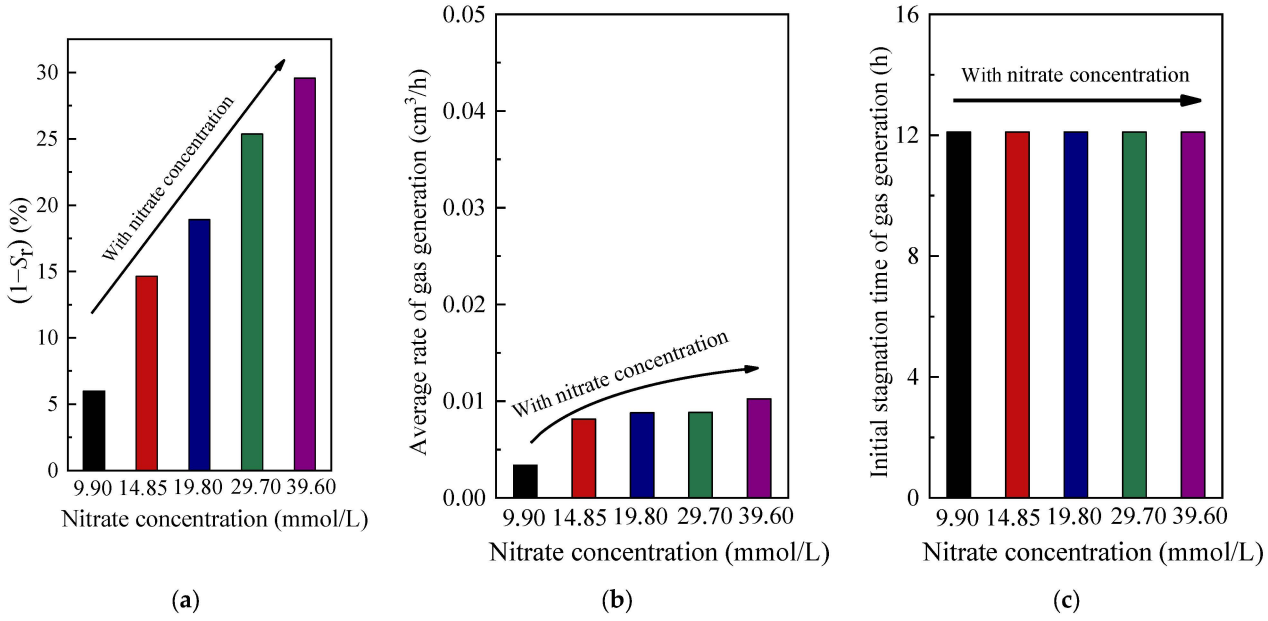

Figure 9. Desaturation curves with different nitrate concentrations (TOC = 1224 mg/L). (**a**) $(1 - S_r)$, (**b**) average rate of gas generation, (**c**) initial stagnation of gas generation.

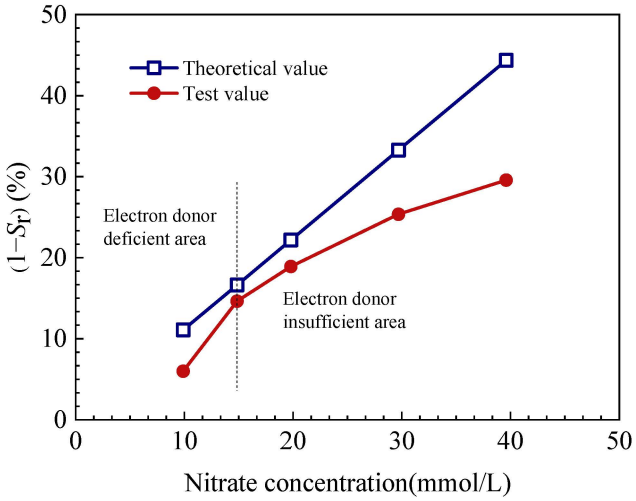

Figure 10. Theoretical and test values of desaturation with different nitrate concentrations.

The C/N is the key parameter that influences the denitrification and efficiency of biogas generation, so it was applied as the index to control the reduction in saturation. Figure 11 shows the relationship between the reduction in saturation and C/N. Figure 11 shows that the reduction in saturation was in a good linear relationship with the C/N. The equation of the relationship satisfied is $1 - S_r = 36.76 - 1.42 \times$ C/N. The value of the fit metric is 0.97. The results of previous related studies further verified this empirical relationship [28]. This result may have been due to the different types of bacteria, electron donor concentrations, slopes, and intercept relation curves. However, the linear relationship showed no change.

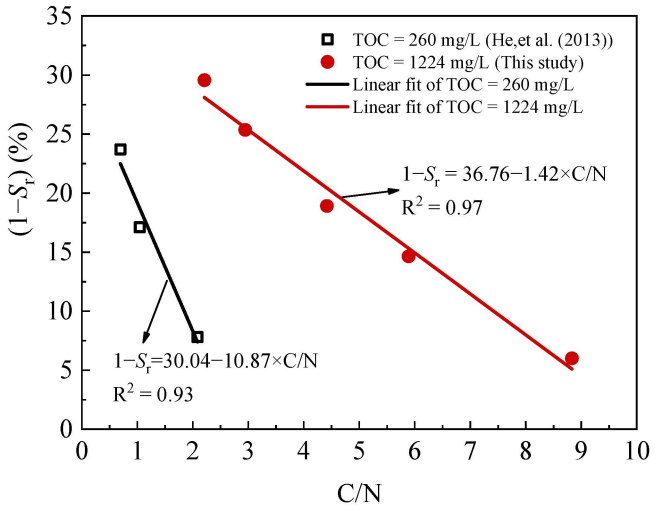

Figure 11. The curves between reduction in saturation versus the carbon–nitrogen ratio [28].

3.3. Influencing Factors of the Degree of Saturation Reduction

3.3.1. Temperatures

Figure 12 illustrates the variations in the parameters of gas generation at different temperatures. The figure shows that the bacteria generated gas between 4 °C and 30 °C. With the increases in temperature, the degree of saturation reduction slightly increased. However, the rate of gas generation significantly increased, and the initial stagnation period decreased sharply. Furthermore, the average gas generation rates were 0.0367 and 0.0089 cm^3/h at 20 °C and 4 °C, respectively. Compared with the latter, the former increased by 4.12-fold. The initial stagnation of gas generation in the sand with temperatures between 4 °C and 15 °C appeared at 18 and 12 h, respectively.

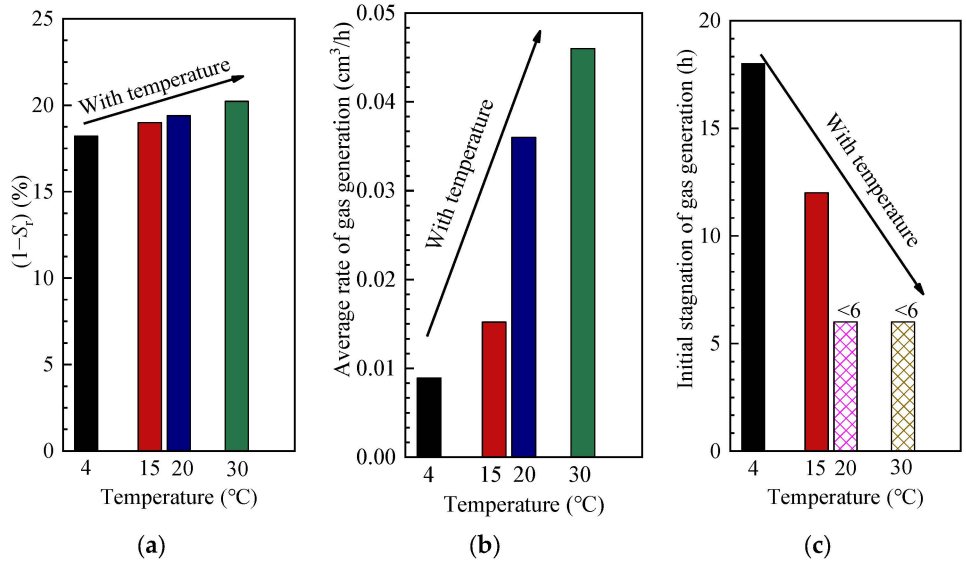

Figure 12. Variations in the parameters of gas generation at different temperatures. (**a**) (1 − S_r), (**b**) average rate of gas generation, (**c**) initial stagnation of gas generation.

The temperature is an important factor that affects protein structure and synthesis. Proteins are the basic component of bacteria. The enzymes that play essential catalytic roles in the process of denitrification are also proteins. When the temperature is low, protein synthesis occurs slowly. Therefore, the growth and metabolic activities of the bacteria were blocked, and the reductase activity of denitrification was low [41]. These factors resulted in inadequate and slow denitrification. Therefore, the degree of saturation

reduction was as low as the rate of gas generation. In addition, *Pseudomonas stutzeri* is a type of facultative anaerobic denitrifying bacterium that conducts aerobic respiration under aerobic environmental conditions and denitrification under anaerobic environmental conditions to produce energy. Given the low metabolic and reductase activities of the bacterium, the time frames for consuming dissolved oxygen and initial stagnation of the gas generation were longer. Therefore, with consideration given to such factors, including the stagnation period and average gas generation rate, the optimum temperatures were 20 °C and 30 °C.

3.3.2. pH

Figure 13 illustrates the variation in the parameters of gas generation and the final pH with different initial pH. As shown in Figure 13, the reduction in saturation reached up to 19.77% when the initial pH was 5. As illustrated in Equation (1), carbon dioxide was the type of biogas produced by denitrification. Given that sand pores formed a relatively closed system, carbon dioxide was trapped inside the pores, and two reversible ionization reactions were observed in the pore water, as shown by Equations (6) and (7):

$$CO_2 + H_2O \rightleftharpoons H^+ + HCO_3^- \quad (6)$$

$$HCO_3^- \rightleftharpoons H^+ + CO_3^{2-} \quad (7)$$

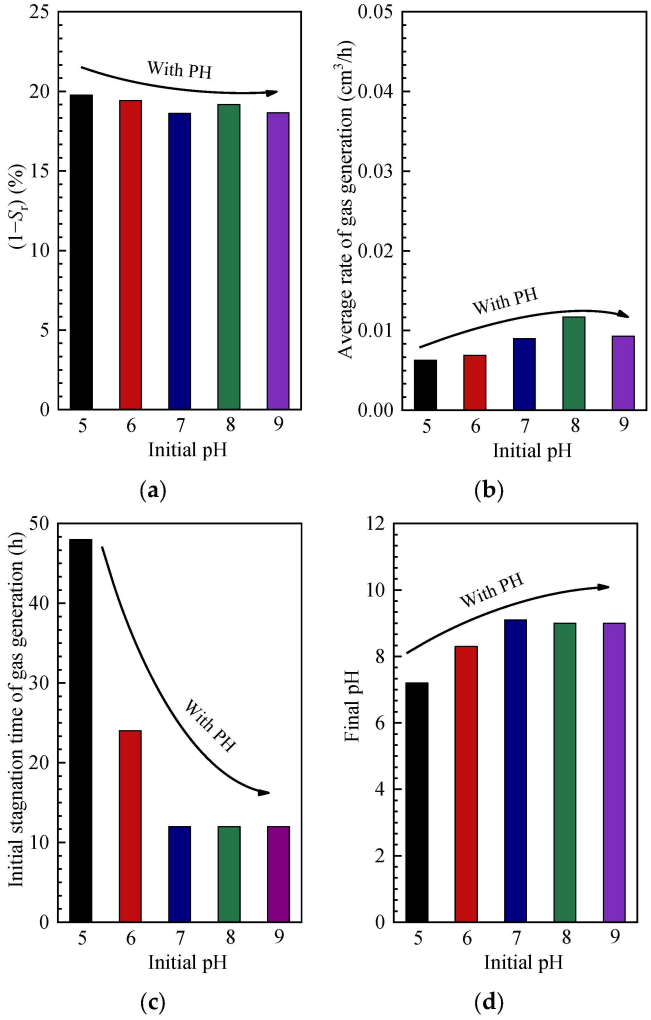

Figure 13. Variations in parameters of gas generation with different initial pH. (**a**) $(1 - S_r)$, (**b**) average rate of gas generation, (**c**) initial stagnation of gas generation, (**d**) final pH.

Carbon exists in the water in three forms, namely, free state, bicarbonate radical, and carbonate. When the pH was increased, the equilibrium of Equations (6) and (7) shifted to the left, and the free state content decreased. When the pH was 5, 6, 7, 8, and 9, the amount of carbon in the free state accounted for 0.957, 0.692, 0.183, 0.028, and 2.142×10^{-3} of the total carbon content, respectively [42]. Figure 9 illustrates the variation in the final pH with different initial pH. Figure 13 shows that denitrification increased the pH of pore water. However, compared with the alkali samples, the final pH of the acidic samples was still low. In the acidic environment, the final degree of saturation was lower. Possibly, a part of the free state CO_2 was not dissolved in pore water. Therefore, the final degree of saturation of the samples reduced slightly as the pH decreased.

The average gas generation rate decreased as the pH decreased. The initial stagnation of gas generation is 48 h when the value of pH is 5. It is only half when pH is 6. In neutral and alkaline conditions, the initial stagnation period is a quarter of acidic conditions. According to the results of related studies [43], nitrate reduction during denitrification is inhibited when the pH is less than or equal to 7. When the pH is between 7 and 9, reduction is not inhibited. However, a cumulative process was evident for nitrites, which would eventually become completely reduced [43]. Figure 13 shows that denitrification can potentially improve the pH of pore water, and the effects of acid inhibition of denitrification on acidity gradually weakened or disappeared. The bacteria gradually developed the capability to produce gas, which slowed down the gas generation rate, and the initial stagnation was prolonged when the initial pH was decreased. Considering the gas generation conditions of various sands under different pH conditions, the most suitable pH of this method was between 7 and 9.

3.3.3. Soils

Figure 14 shows the contrast of samples before and after gas generation. Figure 15 illustrates the variation in the parameters of gas generation with different weight percentages of silt. The figure also shows that the variation in the degree of saturation increased slightly with the increase in silt content. The average rate of gas generation also increased with the increase in silt content. When the silt content was 0%, the average rate of gas generation was 0.009 cm^3/h. When the silt content was 10%, the average rate of gas generation in the sand per cm^3 was 0.030 cm^3/h, which is 3.33 times that of the pure sand. For the initial stagnation, a decrease was observed with the increase in silt content.

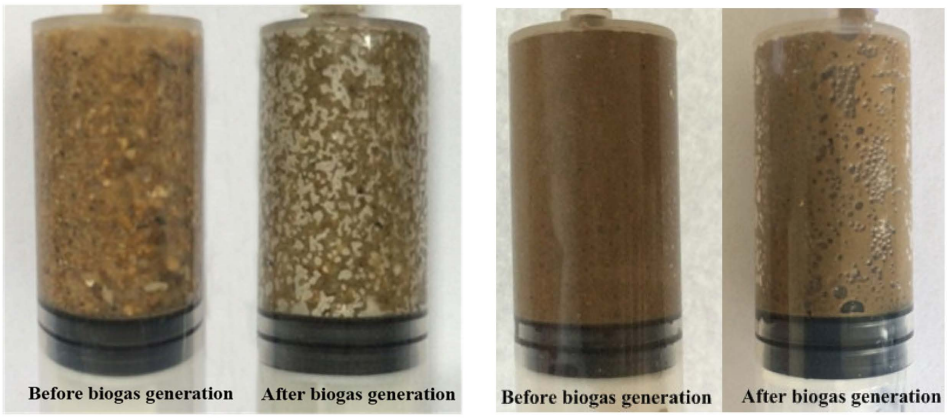

(**a**) (**b**)

Figure 14. Contrast of samples before and after gas generation. (**a**) 100% sand, (**b**) 75% sand + 25% silt.

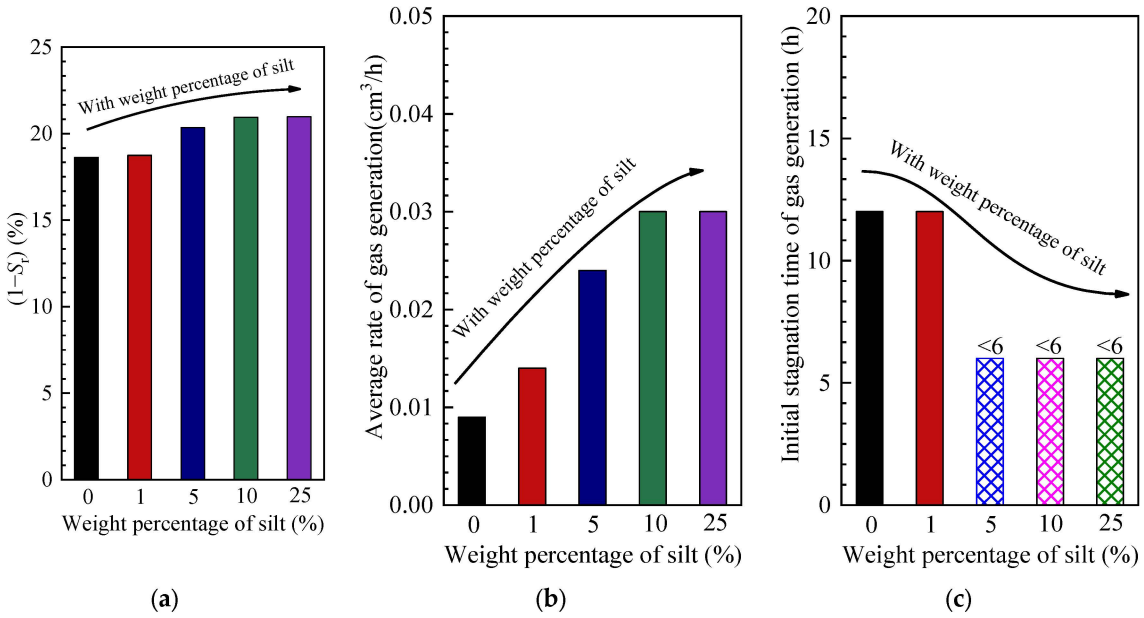

Figure 15. Variations in the parameters of gas generation with different weight percentages of silt. (**a**) (1 − S_r), (**b**) average rate of gas generation, (**c**) initial stagnation of gas generation.

As a product of denitrification reaction, a portion of biogas existed in the form of a dissolved phase in pore water. If its concentration decreases, then denitrification can be promoted [44]. In addition, the dissolved concentration of biogas is related to the soil type. Biogas will dissolve in the fluid until the fluid reaches a supersaturation threshold, which will prompt the homogeneous nucleation of bubbles in the single water phase [45]. However, when a mineral surface exists, the dissolved phase biogas will undergo heterogeneous bubble nucleation at a substantially low supersaturation threshold [42]. The increase in silt content increases the specific surface area of soil particles, providing more available nucleation sites. The supersaturation threshold decreased with the increase in silt weight percentage, and the dissolved concentration of biogas also decreased. Thus, the research results confirmed that denitrification had been promoted. Therefore, the degree of saturation reduction increased, and the initial stagnation period decreased, consistent with the test results of previous related studies [39]. The microbial-induced desaturation for sandy soils containing silt is still effective, not just for clean sand. Compared with 100% sand, increasing the silt content can reduce the initial stagnation, increase the average gas production rate, and increase the reduction in saturation.

3.4. Advantages of Pseudomonas stutzeri

Pseudomonas denitrificans is commonly applied to IPS. However, several practical problems must be addressed for its application in engineering. Firstly, the component of denitrifying cultivation includes eight kinds of compounds, and the carbon source is ethanol, which is volatile and combustible. Secondly, the initial stagnation period of gas generation is long, and the average rate of gas generation is slow, which can decrease the conversion of nitrate. These effects are attributed to two main reasons. The first reason is that the ionic concentration difference between the treatment liquid and pore water can result in ion diffusion, which will retard bacterium growth and denitrification. The other reason is that groundwater seepage accelerates the decrease in ionic concentration in the treatment liquid.

In this study, the formula for denitrifying the culture medium was simple, and all chemical components were non-volatile and noncombustible. Table 4 shows the comparison of *Pseudomonas denitrificans* and *Pseudomonas stutzeri* in terms of the major parameters of the gas generation test. In addition, the gas generation test using *Pseudomonas denitrificans* was conducted in Singapore [28]. Given that the temperature of Singapore is above 20 °C

all year, the 20 °C sample in Study #3 was selected. The bacterial suspension in this study can improve the average rate of gas generation, decreasing the initial stagnation of gas generation. Table 4 also indicates that the key factors affecting the initial stagnation phase and average gas generation rate may be bacteria, the culture medium, the initial density of bacteria, and sand type. However, it indicates the need for further research to optimize the initial condition in the future.

Table 4. Test conditions and contrast results of gas generation tests.

Bacteria	Test Conditions			Test Results		
	Initial OD_{600}	Initial Nitrate Concentration (mmol/L)	Temperature (°C)	Initial Stagnation (h)	Average Rate of Gas Generation of 1 cm^3 Soil (cm^3/h)	Degree of Saturation (%)
Pseudomonas stutzeri	0.100	20.17	20	<3	0.0037	80.81
Pseudomonas denitrificans	0.005	26.74	Room temperature	39	0.0017	76.50

3.5. Mitigate Structure Settlement Using Pseudomonas stutzeri Biogas

It can be observed that desaturation using *Pseudomonas stutzeri* biogas can mitigate the displacement of the building. The building collapsed due to excessive displacement in the fully saturated sandy soil. The building shook violently at the beginning of loading. The sandy soil rises on both sides of the building, and a large amount of water appears around it. However, when microbial-induced desaturation occurred, no water was observed on the foundation surface and the building remained upright.

The settlement time course curves at different saturations are shown in Figure 16. The building of the fully saturated sand foundation showed excessive settlement of 80 mm after the end of loading. This was due to the liquefaction of the fully saturated sand. The effective stress between soil particles is close to 0 and the shear strength of the soil is reduced. However, the settlement after *Pseudomonas stutzeri* biogas desaturation was greatly reduced. The settlement of saturation of 92.5% sand foundation reached 17.1 mm, and the 85% saturation was only 10.6 mm. It can be seen that the reduction in saturation makes the settlement reduced by 86.7%. This indicates that microbial gas-desaturated sand can significantly reduce the settlement of the building, and this technique can be applied to the disposal of liquefied foundations under buildings.

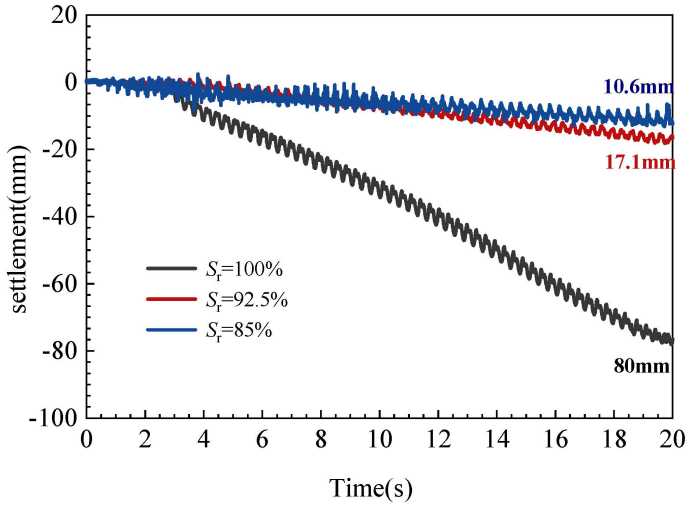

Figure 16. Settlement time course curves at different saturations.

4. Conclusions

Pseudomonas stutzeri was applied to IPS to improve the practicability of desaturation by biogas. *Pseudomonas denitrificans* can effectively decrease the saturation in soil. The specific conclusions were as follows:

(1) The removal rate of nitrate reached 100%. Also, the bacteria proliferate quickly and have a strong denitrification effect when sodium citrate is used as a carbon source. The best carbon source in the denitrification process of *Pseudomonas stutzeri* is sodium citrate. When the OD_{600} of the bacterial suspension was 0.1, the fastest gas generation of microorganisms in the soil pore was observed. In addition, the degree of saturation reduction was the maximum, which indicated that the best bacterial concentration of the bacterium suspension can be used as 0.1.

(2) The C/N of the bacterium suspension was used as the index to control the degree of saturation reduction. According to the results of the experiment, the degree of saturation reduction exhibited a good empirical linear relationship with the C/N.

(3) The final saturation of the samples increased with the slight rise in temperature. The average gas generation rate of bacteria in the sand increased significantly with the increase in temperature. When the temperatures were 15 °C and 4 °C, the bacteria experienced initial stagnation periods of 12 and 18 h during gas generation, respectively. The optimum temperature of this method was between 20 °C and 30 °C.

(4) The average gas generation rate decreased as the pH decreased. The initial stagnation of gas generation is 48 h when the value of pH is 5. It is only half when pH is 6. In neutral and alkaline conditions, the initial stagnation period is a quarter of that of acidic conditions. The most suitable pH was between 7 and 9.

(5) The heterogeneous nucleation sites also increased with the increase in the silt content of sand, which resulted in a low supersaturating threshold in the fluid of the microbial gas, thus promoting denitrification. Therefore, the changes in the silt content in the sand with the change in the average gas generation rate and the initial stagnation period were significant, but the degree of saturation reduction had increased slightly.

(6) The settlement after *Pseudomonas stutzeri* biogas desaturation was greatly reduced. The settlement of saturation of 92.5% sand foundation reached 17.1 mm, and the 85% saturation was only 10.6 mm.

Author Contributions: M.L.: Writing—original draft, Data curation. D.Z.: Resources, Methodology. Funding, Acquisition. E.P.: Methodology. writing—review and editing. Y.G.: Supervision, visualization. All authors have read and agreed to the published version of the manuscript.

Funding: This work was supported by the National Natural Science Foundation of China (51878158).

Data Availability Statement: The data presented in this study are available on request from the corresponding author. The data are not publicly available due to privacy.

Conflicts of Interest: The authors declare no conflict of interest.

References

1. Zhu, Z.; Dupla, J.C.; Canou, J.; Foerster, E. Experimental study of liquefaction resistance: Effect of non-plastic silt content on sand matrix. *Eur. J. Environ. Civ. Eng.* **2022**, *26*, 2671–2689. [CrossRef]
2. Zhu, Z.; Zhang, F.; Peng, Q.; Dupla, J.C.; Canou, J.; Cumunel, G.; Foerster, E. Assessment of the loading waveform on the cyclic liquefaction resistance with Hostun 31 sand. *Soil Dyn. Earthq. Eng.* **2021**, *150*, 106919. [CrossRef]
3. Wu, L.; Cheng, W.; Zhu, Z. Fractional-Order Elastoplastic Modeling of Sands Considering Cyclic Mobility. *J. Mar. Sci. Eng.* **2021**, *9*, 354. [CrossRef]
4. Zimmaro, P.; Nweke, C.C.; Hernandez, J.L.; Hudson, K.S.; Hudson, M.B.; Stewart, J.P. Liquefaction and Related Ground Failure from July 2019 Ridgecrest Earthquake Sequence. *Bull. Seismol. Soc. Am.* **2020**, *110*, 1549–1566. [CrossRef]
5. Simons, M.; Minson, S.E.; Sladen, A.; Ortega, F.; Jiang, J.L.; Owen, S.E.; Meng, L.S.; Ampuero, J.P.; Wei, S.J.; Chu, R.S. The 2011 magnitude 9.0 Tohoku-Oki earthquake: Mosaicking the megathrust from seconds to centuries. *Science* **2011**, *6036*, 1421–1425. [CrossRef]
6. Asuda, S.; Harada, K.; Ishikawa, K.; Kanemaru, Y. Characteristics of liquefaction in Tokyo Bay area by the 2011 Great East Japan Earthquake. *Soils Found.* **2012**, *52*, 793–810. [CrossRef]

7. Montgomery, J.; Wartman, J.; Reed, A.N.; Gallant, A.P.; Hutabarat, D.; Mason, H.B. Field Reconnaissance Data from GEER Investigation of the 2018 MW 7.5 Palu-Donggala Earthquake. *Data Brief* **2021**, *34*, 106742. [CrossRef]
8. Bhattacharya, S.; Hyodo, M.; Goda, K. Liquefaction of sand in the Tokyo Bay area from the 2011 Tohoku (Japan) earthquake. *Soil Dyn. Earthq. Eng.* **2011**, *31*, 1618–1628. [CrossRef]
9. Ghani, S.; Kumari, S. Liquefaction hazard mitigation using computational model considering sustainable development. In *Risk, Reliability and Sustainable Remediation in the Field of Civil and Environmental Engineering*; Elsevier: Amsterdam, The Netherlands, 2022; pp. 183–196.
10. Ghani, S.; Kumari, S. Reliability analysis for liquefaction risk assessment for the city of Patna, India using hybrid computational modeling. *J. Geol. Soc. India* **2022**, *98*, 1395–1406. [CrossRef]
11. Ghani, S.; Sapkota, S.C.; Singh, R.K.; Bardhan, A.; Asteris, P.G. Modelling and validation of liquefaction potential index of fine-grained soils using ensemble learning paradigms. *Soil Dyn. Earthq. Eng.* **2024**, *177*, 108399. [CrossRef]
12. Ghani, S.; Kumari, S. Prediction of soil liquefaction for railway embankment resting on fine soil deposits using enhanced machine learning techniques. *J. Earth Syst. Sci.* **2023**, *132*, 145. [CrossRef]
13. Hossain, Z.; Abedin, M.Z.; Rahman, M.R.; Haque, N.; Jadid, R. Effectiveness of sand compaction piles in improving loose cohesionless soil. *Transp. Geotech.* **2020**, *26*, 100451. [CrossRef]
14. Sadrekarimi, A.; Ghalandarzadeh, A. Evaluation of gravel drains and compacted sand piles in mitigating liquefaction. *Proc. Inst. Civ. Eng. Ground Improv.* **2005**, *9*, 91–104. [CrossRef]
15. Zhao, L.; Chen, Y.; Chen, W.; Wang, J.; Ren, C. The performance of T-shaped deep mixed soil cement column-supported embankments on soft ground. *Constr. Build. Mater.* **2023**, *369*, 130578. [CrossRef]
16. Yoshimi, Y.; Tanaka, K.; Tokimatsu, K. Liquefaction resistance of a partially saturated sand. *Soils Found.* **1989**, *29*, 157–162. [CrossRef] [PubMed]
17. Okamura, M.; Takebayashi, M.; Nishida, K.; Fujii, N.; Jinguji, M.; Imasato, T.; Yasuhara, H.; Nakagawa, E. In-Situ desaturation test by air injection and its evaluation through field monitoring and multiphase flow simulation. *J. Geotech. Geoenviron. Eng.* **2011**, *137*, 643–652. [CrossRef]
18. Okamura, M.; Teraoka, T. Shaking table tests to investigate soil desaturation as a liquefaction countermeasure. *Seism. Perform. Simul. Pile Found.* **2006**, *145*, 282–293.
19. Yegian, M.K.; Eseller-Bayat, E.; Alshawabkeh, A.; Ali, S. Induced-partial saturation for liquefaction mitigation: Experimental investigation. *J. Geotech. Geoenviron. Eng.* **2007**, *133*, 372–380. [CrossRef]
20. He, J.; Chu, J.; Wu, S. Mitigation of soil liquefaction using microbially induced desaturation. *J. Zhejiang Univ. Sci. A* **2016**, *17*, 577–588. [CrossRef]
21. Tsukamoto, Y.; Kawabe, S.; Matsumoto, J.; Hagiwara, S. Cyclic resistance of two unsaturated silty sands against soil liquefaction. *Soils Found.* **2014**, *54*, 1094–1103. [CrossRef]
22. Mele, L.; Tian, J.; Lirer, S.; Lora, A.; Koseki, J. Liquefaction resistance of unsaturated sands: Experimental evidence and theoretical interpretation. *Géotechnique* **2019**, *69*, 541–553. [CrossRef]
23. Zeybek, A.; Madabhushi, S.P.G. Influence of air injection on the liquefaction-induced deformation mechanisms beneath shallow foundations. *Soil Dyn. Earthq. Eng.* **2017**, *97*, 266–276. [CrossRef]
24. Zeybek, A.; Madabhushi, S.P.G. Centrifuge testing to evaluate the liquefaction response of air-injected partially saturated soils beneath shallow foundations. *Bull. Earthq. Eng.* **2017**, *15*, 339–356. [CrossRef]
25. Zeybek, A.; Madabhushi, G.; Santana, P. Durability of partial saturation to counteract liquefaction. *Proc. Inst. Civ. Eng. Ground Improv.* **2017**, *170*, 102–111. [CrossRef]
26. Eseller-Bayat, E.; Yegian, M.K.; Alshawabkeh, A. Liquefaction Response of Partially Saturated Sands. I: Experimental Results. *J. Geotech. Geoenviron. Eng.* **2013**, *139*, 863–871. [CrossRef]
27. He, J.; Chu, J. Undrained Responses of Microbially Desaturated Sand under Monotonic Loading. *J. Geotech. Geoenviron. Eng.* **2014**, *140*, 4014003. [CrossRef]
28. He, J.; Chu, J.; Ivanov, V. Mitigation of liquefaction of saturated sand using biogas. *Géotechnique* **2013**, *63*, 267–275. [CrossRef]
29. Moug, D.M.; Sorenson, K.R.; Khosravifar, A.; Preciado, M.; Stallings Young, E.; Van Paassen, L.; Wang, Y. Field trials of microbially induced desaturation in low-plasticity silt. *J. Geotech. Geoenviron. Eng.* **2022**, *148*, 05022005. [CrossRef]
30. Stallings Young, E.G.; Mahabadi, N.; Zapata, C.E.; Van Paassen, L.A. Microbialinduced desaturation in stratified soil conditions. *Int. J. Geosynth. Ground Eng.* **2021**, *7*, 37. [CrossRef]
31. Li, Y. *Mitigation of Sand Liquefaction Using In Situ Production of Biogas with Biosealing*; Iowa State University: Ames, IA, USA, 2014.
32. Yang, X.; Wang, S.; Zhou, L. Effect of carbon source, C/N ratio, nitrate and dissolved oxygen concentration on nitrite and ammonium production from denitrification process by Pseudomonas stutzeri D6. *Bioresour. Technol.* **2012**, *104*, 65–72. [CrossRef]
33. Peng, E.; Zhang, D.; Sun, W.; Du, G. Desaturation for Liquefaction Mitigation Using Biogas Produced by Pseudomonas stutzeri. *J. Test. Eval.* **2018**, *46*, 20170435. [CrossRef]
34. Peng, E.; Sheng, Y.; Hu, X.; Zhang, D.W.; Hou, Z. Mitigation of sand liquefaction under static loading condition using biogas bubbles generated by denitrifying bacteria. *J. Environ. Manag.* **2021**, *295*, 113106. [CrossRef]
35. Peng, E.; Sheng, Y.; Hu, X.; Zhang, D. Undrained Responses of Partially Saturated Sand Induced by Biogas under Dynamic Cyclic Loading. *J. Test. Eval.* **2021**, *49*, 20190841. [CrossRef]

36. Peng, E.; Hou, Z.; Sheng, Y.; Zhang, D.; Song, L.; Chou, Y.L. Anti-liquefaction performance of partially saturated sand induced by biogas under high intensity vibration. *J. Clean. Prod.* **2021**, *319*, 128794. [CrossRef]
37. Henderson, S.L.; Dandie, C.E.; Goyer, C.; Zebarth, B.J.; Burton, D.L.; Trevors, J.T.; Gilkes, R.J.; Prakongkep, N. Glucose effects on denitrifier abundance, denitrification gene mRNA levels, and denitrification activity in an anoxic soil microcosm. In Proceedings of the 19th World Congress of Soil Science, Brisbane, QL, Australia, 1–6 August 2010.
38. Philippot, L.; Andert, J.; Jones, C.M.; Bru, D.; Hallin, S. Importance of denitrifiers lacking the genes encoding the nitrous oxide reductase for N_2O emissions from soil. *Glob. Change Biol.* **2011**, *17*, 1497–1504. [CrossRef]
39. Rebatalanda, V.; Santamarina, J.C. Mechanical effects of biogenic nitrogen gas bubbles in soils. *J. Geotech. Geoenviron. Eng.* **2012**, *138*, 128–137. [CrossRef]
40. Cole, J.A.; Brown, C.M. Nitrite reduction to ammonia by fermentative bacteria: A short circuit in the biological nitrogen cycle. *FEMS Microbiol. Lett.* **1980**, *7*, 65–72. [CrossRef]
41. Carrera, J.; Vicent, T.; Lafuente, F.J. Influence of temperature on denitrification of an industrial high-strength nitrogen wastewater in a two-sludge system. *Water Sa* **2003**, *29*, 11–16. [CrossRef]
42. Gerven, T.V.; Baelen, D.V.; Dutré, V.; Vandecasteele, C. Influence of carbonation and carbonation methods on leaching of metals from mortars. *Cem. Concr. Res.* **2004**, *34*, 149–156. [CrossRef]
43. Glass, C.; Silverstein, J.A. Denitrification kinetics of high nitrate concentration water: PH effect on inhibition and nitrite accumulation. *Water Res.* **1998**, *32*, 831–839. [CrossRef]
44. Senbayram, M.; Chen, R.; Budai, A.; Bakken, L.; Dittert, K. N_2O emission and the $N_2O/(N_2O+N_2)$ product ratio of denitrification as controlled by available carbon substrates and nitrate concentrations. *Agric. Ecosyst. Environ.* **2012**, *147*, 4–12. [CrossRef]
45. Ronen, D.; Berkowitz, B.; Magaritz, M. The development and influence of gas bubbles in phreatic aquifers under natural flow conditions. *Transp. Porous Media* **1989**, *4*, 295–306. [CrossRef]